

- ²⁵H. Stanton, Ph.D. thesis (Brown University, 1969) (unpublished).
²⁶I. Gerstein and C. Elbaum (unpublished).
²⁷R. J. von Gutfeld, in *Physical Acoustics*, edited by W. P. Mason (Academic, New York, 1968), Vol. 5, p. 233.
²⁸B. Taylor, H. J. Maris, and C. Elbaum, *Phys. Rev. B* **3**, 1462 (1971).
²⁹B. Taylor, Ph.D. thesis (Brown University, 1970) (unpublished).
³⁰H. J. Maris, *J. Acoust. Soc. Am.* **50**, 812 (1970).
³¹J. J. Hall, *Phys. Rev.* **128**, 68 (1962).
³²A. M. Glass, *Can. J. Phys.* **43**, 12 (1965).
³³I. Balselev, *Solid State Commun.* **5**, 315 (1967).
³⁴F. H. Pollak and M. Cardona, *Phys. Rev.* **172**, 816 (1968).
³⁵R. L. Jones and P. Fisher, *Phys. Rev. B* **2**, 2016 (1970).
³⁶L. D. Laude, F. H. Pollak, and M. Cardona, *Phys. Rev. B* **3**, 2623 (1970).
³⁷I. Balselev, *Phys. Rev.* **143**, 636 (1966).
³⁸I. P. Akimchenko and V. A. Vdovenkov, *Fiz. Tverd. Tela* **11**, 658 (1969) [*Sov. Phys.-Solid State* **11**, 528 (1969)].
³⁹R. Truell, C. Elbaum, and B. B. Chick, *Ultrasonic Methods in Solid State Physics* (Academic, New York, 1969).

PHYSICAL REVIEW B

VOLUME 7, NUMBER 4

15 FEBRUARY 1973

Calculation of the Thermal Expansion for a Quasiharmonic Model of Tellurium*

T. G. Gibbons

*Division of Chemistry, National Research Council of Canada,
Ottawa, Ontario, Canada K1A 0R6*

(Received 2 June 1972)

A simple quasiharmonic model, employing a valence-force approach, is used to calculate the Grüneisen functions and thermal expansion of tellurium. The calculations illustrate the use of a new thermodynamic formalism for treating internal strain and reveal explicitly the effect that an internal degree of freedom has upon the macroscopic properties. The valence-force picture of tellurium is critically discussed in the light of a comparison of the calculations with experiment. Suggestions are made for further experimental work and for improvements in the theoretical model.

I. INTRODUCTION

The present paper is concerned with the application of quasiharmonic theory to calculate the Grüneisen functions and thermal expansion for a simple lattice-dynamical model of tellurium. The structure of tellurium consists of parallel helical chains of atoms, disposed in an hexagonal array, and belongs to the space group D_3^4 or D_3^6 (see Fig. 1), in the Schoenflies notation, equivalent to $P3_121$ or $P3_221$ in the Hermann-Mauguin notation, where the alternatives represent helices of opposite handedness. The neighboring element in group VIb, selenium, also has this structure but the present calculations are applied specifically to tellurium since this has been far more widely studied experimentally.

A considerable amount of experimental data are available for comparison with "harmonic" lattice models. The zone-center optic frequencies have been measured by infrared^{1,2} and, more recently, Raman studies.^{3,4} Using coherent neutron scattering, Powell and Martel⁵ have measured phonon dispersion curves along certain high-symmetry directions and their measurements correlate well with the optical measurements, and also with frequency spectra obtained from earlier neutron work of Kotov *et al.*⁶ and Gissler and Axmann⁷ (although the former's value for the highest-frequency peak appears to be a little high). Data also exist for the

elastic constants⁸ between 100 and 300 °K and the specific heat⁹⁻¹¹ down to 1 °K.

The thermal-expansion coefficients of α_{\perp} and α_{\parallel} of tellurium have been measured by a variety of techniques¹²⁻¹⁷ at temperatures from 2 up to 500 °K, and the different measurements are in reasonably close agreement with each other. The data have been analyzed in terms of the Grüneisen functions γ_{\perp} and γ_{\parallel} , and, as for the thermal expansion, the behavior is strongly anisotropic. The tellurium structure retains an internal degree of freedom during thermal expansion so that an internal expansion coefficient can also be measured.¹⁵

Before applying quasiharmonic theory to calculate the thermal expansion it was necessary to begin with a harmonic model which was reasonably compatible with experiment but which allowed anharmonicity to be introduced in a straightforward and meaningful way. For this reason a model was chosen based on that of Hulin¹⁸ and using a force field approach similar to the models put forward by Geick and Schröder¹⁹ and Nakayama *et al.*²⁰ The shortcomings of these models are pointed out but they are preferable to the more successful model of Pine and Dresselhaus⁴ which involves too many adjustable parameters and is too generalized for present purposes.

As mentioned above, when tellurium expands on heating it maintains an internal degree of freedom.

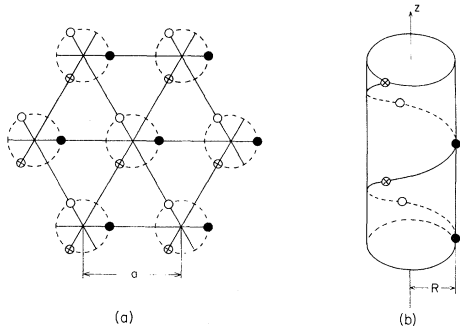


FIG. 1. (a) View of the tellurium structure looking down the trigonal z axis (after Hulin, Ref. 18). Atoms are distinguished according to their projections along this axis: \bullet , in plane; \circ , $\frac{1}{3}c$ above plane; \otimes , $\frac{2}{3}c$ above plane. (b) Side view of a section of one helical chain (after Hulin, Ref. 18).

For the purposes of calculation, this situation requires a thermodynamic treatment in which both external and internal strains are treated on the same footing. The necessary thermodynamic formalism has been presented and specifically applied to the tellurium structure in an earlier paper.²¹ In Sec. II the aspects of this formalism relevant to the present work are summarized.

Sections III and IV deal with a description of the lattice model and outline the method of calculation. In Sec. V the behavior of the harmonic model employed as a basis for the quasiharmonic calculations is compared with experimental measurements of the phonon dispersion curves, the harmonic-frequency spectrum, elastic constants, and specific heat. In Sec. VI the calculated Grüneisen functions and thermal-expansion coefficients are presented as functions of temperature for a very simple anharmonic model and the results are compared with experiment.

In Sec. VII the valence-force approach used in the present work is critically discussed and suggestions are made for improving the model and for further experimental work.

II. PRELIMINARY THEORY

In a thermodynamic treatment of thermal expansion under isotropic (in this case, zero) pressure, only strains which preserve the full crystal symmetry need be considered. For the tellurium structure, as for all axial crystals, there are only two such external strains; a uniform extension in all directions perpendicular to the unique axis, and an extension along this axis. Corresponding strain coordinates are conveniently defined for the purposes of calculation by

$$\eta_a = (a - a^0)/a^0, \quad \eta_c = (c - c^0)/c^0, \quad (1)$$

where a and c are the hexagonal-unit-cell parameters

and the zero superscript denotes evaluation at the reference configuration. Retention of crystal symmetry in the tellurium structure also allows one internal degree of freedom and hence one internal strain coordinate is required. This is denoted by ϵ_R as it is conveniently defined in terms of the radius R of the helical chains,

$$\epsilon_R = (R - R^0)/R^0. \quad (2)$$

The three symmetry-preserving strain coordinates, η_a , η_c , and ϵ_R form the basis for a "general thermodynamic regime" in which all three coordinates are treated as independent variables. All thermodynamic quantities calculated from the theoretical model presented later belong to this regime, and they must then be related to quantities measured experimentally. The thermodynamic relationships involved have been presented in detail for the tellurium structure in an earlier paper²¹ and will only be summarized here. The same notation will be used, i.e., capital script letters denote quantities in the general regime and capital italic subscripts refer to the complete set of external and internal coordinates. For example \mathcal{G}_A ($A = a, c, R$) represents the strains η_a , η_c , and ϵ_R . \mathcal{T}_A represents the corresponding conjugate stresses, defined by considering the work done through the symmetry-preserving coordinates

$$d\mathcal{W} = V^0 \mathcal{T}_A d\mathcal{G}_A, \quad (3)$$

where V^0 is the volume in the reference configuration and the Einstein summation convention is used. The Helmholtz energy \mathcal{F} and Gibbs energy \mathcal{G} are defined in a manner analogous to normal "macroscopic" thermodynamics

$$\mathcal{U} - T\mathcal{S} = \mathcal{F} = \mathcal{G} + V^0 \mathcal{T}_A \mathcal{G}_A. \quad (4)$$

The three thermal expansion coefficients α_A ($A = a, c, R$) comprise the two external expansion coefficients, written more commonly as α_\perp and α_\parallel , and an internal expansion coefficient

$$\alpha_\perp = \left(\frac{\partial \eta_a}{\partial T} \right)_T, \quad \alpha_\parallel = \left(\frac{\partial \eta_c}{\partial T} \right)_T, \quad \alpha_R = \left(\frac{\partial \epsilon_R}{\partial T} \right)_T. \quad (5)$$

These can be calculated theoretically by means of the relation

$$\alpha_A = \mathcal{C}_\mathcal{G}^T \mathcal{S}_{AB}^T \Gamma_B / V^0, \quad (6)$$

where $\mathcal{C}_\mathcal{G}$ is the heat capacity at constant external and internal strain, \mathcal{S}_{AB}^T is an isothermal elastic compliance obtained as the inverse of the matrix \mathcal{C}_{AB}^T , comprising six independent elastic stiffnesses exemplified by

$$\mathcal{C}_{aR}^T = \frac{1}{V^0} \left(\frac{\partial^2 \mathcal{F}}{\partial \eta_a \partial \epsilon_R} \right)_{c,T} = \mathcal{C}_{Ra}^T, \quad (7)$$

and Γ_B represents the three Grüneisen functions

$$\Gamma_a = \frac{1}{c_g} \left(\frac{\partial s}{\partial \eta_a} \right)_{c,R,T}, \quad \Gamma_c = \frac{1}{c_g} \left(\frac{\partial s}{\partial \eta_c} \right)_{a,R,T}, \quad (8)$$

$$\Gamma_R = \frac{1}{c_g} \left(\frac{\partial s}{\partial \epsilon_R} \right)_{a,c,T}.$$

The more familiar Grüneisen functions and elastic constants in the "macroscopic regime" are obtained through the relations

$$\gamma_{\perp} = \frac{c_g}{2C_{\eta}} \left(\Gamma_a - \frac{\Gamma_R c_{Ra}^T}{c_{RR}^T} \right), \quad (9)$$

$$\gamma_{\parallel} = \frac{c_g}{C_{\eta}} \left(\Gamma_c - \frac{\Gamma_R c_{Rc}^T}{c_{RR}^T} \right), \quad (10)$$

$$\frac{C_{\eta}}{c_g} = 1 + \frac{T c_g \Gamma_R^2}{V^0 c_{RR}^T}, \quad (11)$$

$$2(c_{11}^T + c_{12}^T) = c_{aa}^T = c_{aa}^T - (c_{Ra}^T)^2 / c_{RR}^T, \quad (12)$$

$$c_{33}^T = c_{cc}^T = c_{cc}^T - (c_{Rc}^T)^2 / c_{RR}^T, \quad (13)$$

$$2c_{13}^T = c_{ac}^T = c_{ac}^T - c_{aR}^T c_{cR}^T / c_{RR}^T. \quad (14)$$

The second terms in the right-hand side of these equations arise due to the "internal relaxation" which occurs when the constraint of constant chain radius is lifted. Notice that the macroscopic Grüneisen functions γ_{\perp} and γ_{\parallel} do not depend purely on the anharmonic part of the lattice potential as they do in crystals with no internal degrees of freedom. This is because the internal elastic properties are involved in determining the degree of internal relaxation. It is the Γ_A which are now the purely "anharmonic" quantities.

For η_a , η_c , and ϵ_R defined as in Eqs. (1) and (2) the left-hand-side equalities in Eqs. (12)–(14) only hold if evaluated at the reference configuration and for zero stress. This is the case for all the calculations presented later. Results for the theoretical model show that the ratio C_{η}/c_g used in Eqs. (9) and (10) is within 0.05% of unity even at temperatures well above Θ_0 .

III. LATTICE MODEL

The model employs potentials analogous to those of the Hulin model, and these are written as $\phi_i(r_i)$, $\phi_b(r_b)$, and $\phi_{\theta}(\cos\theta)$, where r_i is the "in-chain" distance between nearest neighbors, r_b is the "between-chain" distance between next nearest neighbors, and θ is the angle between adjacent bonds in a chain (see Fig. 1). "Tensions" t , "force constants" k , and dimensionless "anharmonicities" A are defined from derivatives of these potentials:

$$t_i = \phi_i'(r_i)/r_i, \quad k_i = \phi_i''(r_i), \quad A_i = r_i \phi_i'''(r_i)/\phi_i''(r_i), \quad (15)$$

$$t_b = \phi_b'(r_b)/r_b, \quad k_b = \phi_b''(r_b), \quad A_b = r_b \phi_b'''(r_b)/\phi_b''(r_b), \quad (16)$$

$$t_{\theta} = \phi_{\theta}'(\cos\theta)/r_i^2, \quad k_{\theta} = \phi_{\theta}''(\cos\theta)/r_i^2,$$

$$A_{\theta} = \phi_{\theta}'''(\cos\theta)/\phi_{\theta}''(\cos\theta). \quad (17)$$

The primes denote successive orders of differentiation with respect to the arguments and all derivatives are evaluated at the equilibrium values of r_i , r_b , and θ .

These three interactions provide a lattice which is stable against macroscopic deformations. However, to be stable against all small deformations, all the normal-mode frequencies must be real and positive. For simple models which represent the between-chain interactions by a single central-force pair potential of the type $\phi_b(r_b)$ above,^{18–20} some normal-mode frequencies are zero at the Brillouin-zone boundary. Following the suggestion of Geick and Schröder¹⁹ this instability is removed by including a central-force interaction $\phi_a(a)$ between fourth nearest neighbors which occupy adjacent chains and lie in a plane perpendicular to the z axis, at a distance apart given by the lattice parameter a . Potential parameters are defined as before,

$$t_a = \phi_a'(a)/a, \quad k_a = \phi_a''(a), \quad A_a = a \phi_a'''(a)/\phi_a''(a) \quad (18)$$

In all the calculations to be presented, the stress is assumed to be zero in the reference configuration, and hence $t_i = t_b = t_{\theta} = 0$. The normal-mode frequencies in the harmonic approximation are then determined by the force constants k_i , k_b , k_{θ} , and k_a . However, in order to improve the fit to the "harmonic" properties it has proved necessary to introduce second-order harmonic interactions into the valence-force field within the helical chains, hence making them more "molecular" in nature. Two interaction constants are employed: k_{ii} , a force constant describing an interaction between adjacent bonds in a chain, and $k_{i\theta}$, describing an interaction between an in-chain bond and the angle which it forms with an adjacent in-chain bond.

The total strain-energy density of the static lattice, to third order in the potential arguments, and for zero initial stress, then becomes

$$(\Phi - \Phi^0)/V = (1/2v) [3k_i(\delta r_i)^2 + 6k_b(\delta r_b)^2 + 3r_i^2 k_{\theta}(\delta \cos\theta)^2 + 9k_a(\delta a)^2 + 6k_{ii}(\delta r_i)^2 + 12r_i k_{i\theta} \delta r_i \delta \cos\theta + (k_i/r_i) A_i (\delta r_i)^3 + 2(k_b/r_b) A_b (\delta r_b)^3 + r_i^2 k_{\theta} A_{\theta} (\delta \cos\theta)^3 + 3(k_a/a) A_a (\delta a)^3], \quad (19)$$

where Φ is the total static lattice potential and v is the volume of the hexagonal unit cell

$$v = \frac{1}{2} \sqrt{3} a^2 c. \quad (20)$$

Equation (19) serves to define k_{ii} and $k_{i\theta}$. Double differentiation of this expression with respect to the strains η_a , η_c , and ϵ_R yields the elastic stiffnesses c_{AB} defined by Eq. (7) (no superscript T is necessary since in the strict harmonic approxi-

mation the only contribution is from the static lattice potential).

The parameters A_i, A_b, A_θ , and A_a provide contributions purely to the anharmonic part of the total lattice potential (i.e., terms higher than second order in the atomic displacements). They do not therefore enter into calculations of the normal-mode frequencies using the harmonic approximation. (Even when these parameters are zero, the lattice potential is not "harmonic" since the third-order and higher derivatives of the total lattice potential still contain contributions from the first and second derivatives of the individual valence-force potentials.²² In the harmonic approximation, therefore, such higher-order terms are ignored, but not necessarily zero.)

IV. METHOD OF CALCULATION

In the harmonic approximation the normal-mode frequencies $\omega(\vec{q}, s)$ for any allowed wave vector \vec{q} are calculated by solving the secular equation

$$\underline{D}(\vec{q})\vec{e}(\vec{q}, s) = \omega^2(\vec{q}, s)\vec{e}(\vec{q}, s), \quad (21)$$

where the dynamical matrix $\underline{D}(\vec{q})$ is a 9×9 Hermitian matrix (there are three atoms per unit cell and no centers of inversion) and $\vec{e}(\vec{q}, s)$ is the complex eigenvector corresponding to the s th eigenvalue $\omega^2(\vec{q}, s)$, where $s = 1 \dots 9$. $\underline{D}(\vec{q})$ was constructed, using standard Born-von Kármán theory, from the harmonic force constants defined in Sec. III (for more detail of the calculation see Gibbons²³).

The secular equation was solved for points forming a regular mesh over reciprocal space. The "root-sampling" method was then used to obtain the harmonic-frequency spectrum, $G(\omega)$, and integrals over $G(\omega)$ such as the heat capacity c_g :

$$c_g = \sum_{q,s} C(\vec{q}, s). \quad (22)$$

The summation is over all normal modes q, s , and $C(q, s)$ is the heat-capacity contribution from each mode:

$$C(q, s) = \frac{k[\hbar\omega(\vec{q}, s)/kT]e^{\hbar\omega/kT}}{(e^{\hbar\omega/kT} - 1)^2}. \quad (23)$$

In the quasiharmonic approximation the normal-mode frequencies are allowed to be strain dependent. Individual normal-mode Grüneisen parameters are defined to express this strain dependence:

$$\Gamma_A(\vec{q}, s) = - \left(\frac{\partial \ln \omega(\vec{q}, s)}{\partial \epsilon_A} \right)_{g^*}, \quad (A = a, c, R). \quad (24)$$

These were calculated for each point in the integration mesh over reciprocal space, using the first-order perturbation-theory result

$$\Gamma_A(\vec{q}, s) = - \langle \vec{e}^{(0)}(\vec{q}, s) | \underline{D}^{(A)}(\vec{q}) | \vec{e}^{(0)}(\vec{q}, s) \rangle / 2(\omega^{(0)})^2, \quad (25)$$

where (0) specifies zero-order solutions to the secular equation (21) (if the strain lifts a degeneracy, eigenvectors must be taken which are valid in the strained state), and $\underline{D}^{(A)}(\vec{q})$ is the first-order coefficient matrix obtained when $\underline{D}(\vec{q})$ is expanded to first order in each of the symmetry-preserving strains η_a, η_c , and ϵ_R . The phase-dependent quantities $\exp[i(\vec{q} \cdot \vec{r}_i)]$ in $\underline{D}(\vec{q})$ are independent of strain to first order so that each $\underline{D}^{(A)}(\vec{q})$ matrix is completely determined by the first-order strain coefficients of the Born-von Kármán force-constant matrices $\underline{\Phi}(\vec{k})$. These are functions of geometry (a, c, R), tensions (t_i, t_b, t_θ, t_a), and force constants (k_i, k_b, k_θ, k_a), and all these quantities change with strain. Note that although the "tensions" t_i, t_b, t_θ and t_a are zero in the initial configuration they must be included in the expressions for the elements of $\underline{\Phi}(\vec{k})$ since they may become nonzero on straining, to an extent determined by the nature of the strain and the force constant. (This serves to illustrate the point made at the end of Sec. III, i.e., even when A_i, A_b, A_θ , and A_a are zero, the $\underline{D}^{(A)}(\vec{q})$, and hence Γ_A , are nonzero due to contributions from the change in geometry and tensions with strain.)

The thermodynamic Γ_A defined in Eqs. (8) were then obtained as a weighted average over reciprocal space:

$$\Gamma_A = \sum \Gamma_A(\vec{q}, s) C(\vec{q}, s) / c_g. \quad (26)$$

This equation is analogous to that for the more familiar γ_λ in the macroscopic regime.²⁴ The thermal-expansion coefficients $\alpha_\perp, \alpha_\parallel$, and α_R , defined in Eqs. (5), were then obtained using Eq. (6), and γ_\perp and γ_\parallel were calculated by means of Eqs. (9)–(11).

The strain dependence of different regions of the frequency spectrum was also studied in the form of the quantities $\bar{\Gamma}_A(\omega)$, analogous to the $\bar{\gamma}_\nu$ of Blackman,²⁵ which were obtained as a function of frequency by taking the arithmetic mean of the $\Gamma_A(\vec{q}, s)$ of all modes calculated within a small finite frequency interval: Thus if there are P modes in the interval at ω ,

$$\bar{\Gamma}_A(\omega) = \sum_{qs} \Gamma_A(\vec{q}, s) / P. \quad (27)$$

V. HARMONIC PROPERTIES

Apart from the instability which is removed by an additional fourth-neighbor potential $\phi_a(a)$, the basic Hulin model has the disadvantage that it cannot be fit simultaneously to both the elastic and optical data. There are two main discrepancies.

(i) For any reasonable fit of the upper optical branches to experiment, the in-chain force constants k_i and k_θ have to be set to values which make the stiffness of the chains (and hence the elastic constant c_{33}) too low.

(ii) The force constant k_b can be fit exactly to the experimental measurement of the A_2 zone-center frequency since this is a "chain twist" mode whose frequency depends completely upon between-chain forces. However k_b cannot be fit to the A_2 frequency without making the chains too tightly bound so that $(c_{11} + c_{12})$ is too large relative to c_{33} for any reasonable fit of the other parameters.

In consequence, the best fit of the Hulin model to the phonon frequencies leads to the reverse elastic anisotropy [$(c_{11} + c_{12}) > c_{33}$] to that obtained experimentally. This situation is largely overcome and disadvantage (i) is removed by introducing the harmonic interaction parameters k_{ii} and $k_{i\theta}$. These are found to strongly affect the frequencies of the three upper optical branches while leaving the rest of the phonon spectrum essentially unchanged. Relatively large negative values of $k_{i\theta}$ do, however, result in an instability manifested by a zero acoustic frequency. A positive k_{ii} and negative $k_{i\theta}$ both help to "stiffen" the helical chains while lowering the frequency of the upper optical branches. Thus a good fit to these branches can be maintained while higher values of k_i and k_θ are employed to give a reasonable c_{33} . A negative $k_{i\theta}$ also gives rise to a more realistic $c_{13}/(c_{11} + c_{12})$ ratio which is too low in the Hulin model (and which has great influence on the thermal expansion as shown later).

However, apart from improvements to the phonon spectrum and a more realistic elastic anisotropy using the harmonic interactions k_{ii} and $k_{i\theta}$, disadvantage (ii) of the Hulin model still remains. The between-chain interactions are too simply represented. Further improvements require interactions of a more complex nature (see Sec. VII). For the present model therefore, a compromise is attempted in the choice of a value for k_b . The choice of values was also affected to some extent by consideration of the results for the Grüneisen functions and thermal expansion as we shall see later. Table I shows the values chosen for the harmonic force constants and the resulting values of $(c_{11} + c_{12})$, c_{13} , and c_{33} (which are all that are needed for calculating the thermal expansion) compared with experiment. Figure 2 shows the resulting phonon dispersion curves in certain high-symmetry directions together with neutron and optical data. The notation is that of Kittel.²⁶

The harmonic-frequency spectrum is shown in Fig. 3 with the spectrum obtained by Kotov *et al.*⁶ superimposed on it. A noticeable defect of the model appears to be the lack of a decisive band gap at $\sim 1.1 \times 10^{13}$ rad/sec which is also indicated by the results of Powell and Martel.⁵ This is a defect of the Pine and Dresselhaus model⁴ as well as all simpler harmonic models put forward so far. The dependence of different regions of the

TABLE I. Values chosen for the harmonic force constants and the resulting values of $(c_{11} + c_{12})$, c_{13} , and c_{33} compared with experiment.

| Harmonic force constants (in units of 10^4 dyn cm ⁻¹) | | | | | |
|--|-------|------------|----------|---------------------|---------------|
| k_i | k_b | k_θ | k_a | k_{ii} | $k_{i\theta}$ |
| 6.251 | 1.250 | 1.000 | 0.188 | 0.313 | -0.563 |
| Elastic constants for symmetry-preserving strains (in units of 10^{11} dyn cm ⁻²) | | | | | |
| | | c_{33} | c_{13} | $(c_{11} + c_{12})$ | |
| Calculated | | 7.27 | 2.04 | 5.26 | |
| Experimental | | 7.22 | 2.50 | 4.14 | |

frequency spectrum upon the force constants was roughly determined by slightly changing each constant in turn. Regions A-E were distinguished. The highest peak A was strongly dependent upon k_i and hence mainly consists of in-chain bond stretching modes. Regions B and C were more dependent upon k_θ and hence involve a large proportion of angle bending modes. Region D contains acoustic and lower optic "chain torsion" modes dependent mainly upon nearest-neighbor between-chain forces, whereas the lowest peak E is more strongly affected by the fourth-neighbor central force k_a .

The calculated specific heat was found to agree with experiment to within 6% over the whole range of temperature for which experimental values are available.

VI. GRÜNEISEN FUNCTIONS AND THERMAL EXPANSION

The simple harmonic model described in Sec. V was extended to include the four anharmonic parameters A_i , A_b , A_θ , and A_a defined in Sec. III. An investigation was then carried out of how well this simple anharmonic model could reproduce experimental data of the Grüneisen functions and thermal expansion of tellurium. An exact fit could not be obtained but the range of parameters producing reasonable agreement was sufficiently limited for the basic inadequacies of the model to be pinpointed. For the results presented and discussed here, the following values were given to the anharmonic parameters:

$$A_i = 0, \quad A_b = -14, \quad A_a = -19, \quad A_\theta = +3.$$

Therefore, for this particular model the between-chain central interactions are taken to be the most anharmonic (a value of -21 corresponds to a 6-12 potential). Such potentials give positive contributions to the $\Gamma_A(q, s)$ [defined in Eq. (24)] for strains which cause an increase in bond length, since the lowered force constant lowers frequencies dependent upon it. For example, frequencies strongly dependent upon the between-chain force constant k_b would have a large positive $\Gamma_A(\vec{q}, s)$ and a

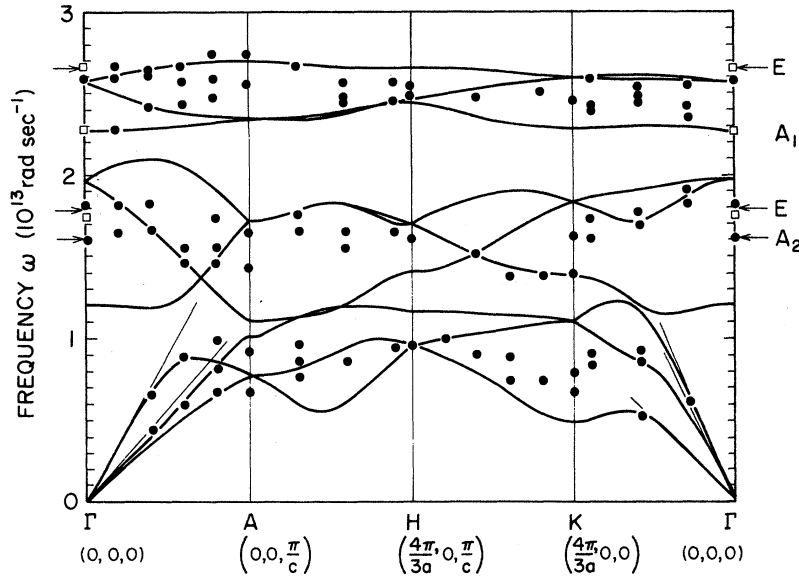


FIG. 2. Calculated phonon dispersion curves (solid lines) in certain high-symmetry directions compared with the neutron measurements (●) of Powell and Martel (Ref. 5), and optical data [□ (Ref. 4); → (Ref. 1)]. Experimental acoustic velocities (Ref. 8) are also shown.

negative $\Gamma_R(\vec{q}, s)$ (the internal strain ϵ_R decreases the r_b distance). The changes in geometry and in the first derivatives of the potentials (tensions) on straining also give rise to contributions to the $\Gamma_A(\vec{q}, s)$; usually negative contributions since these changes tend to raise frequencies.^{27,28} These are the only contributions for Hooke's law potentials (see end of Sec. III) such as the in-chain pair potentials ϕ_i , for which A_i is taken to be zero.

The value of +3 for A_θ corresponds to a slight decrease in the angle force constant k_θ as θ is increased (and hence $\cos\theta$ is decreased). Thus, A_θ gives rise to positive contributions to the $\Gamma_c(\vec{q}, s)$ and negative contributions to the $\Gamma_R(\vec{q}, s)$, particularly for optic frequencies in the middle region of the spectrum since these depend strongly on the angle force constant.

The above arguments, taken in conjunction with the dependence of different regions of the frequency spectrum upon the harmonic force constants (see Sec. V), explain most of the features of the strain dependence of the frequency spectrum, presented in the form of the $\bar{\Gamma}_A(\omega)$ in Fig. 4. The pronounced dip in $\bar{\Gamma}_c(\omega)$ and $\bar{\Gamma}_R(\omega)$ at low frequencies is, however, due to induced tensions. This was deduced because the dip remained when one set $A_i = A_b = A_\theta = A_a = 0$. Evidently, strains η_c and ϵ_R markedly increase the acoustic frequencies in this region of the dip. The modes concerned are probably transverse acoustic propagating along the chains. An increase in r_i , caused by either strain η_c or ϵ_R , would induce strong tensions t_i which would raise these frequencies considerably.

Figure 5 shows a $\log_{10} T$ plot of the thermodynamic Γ_A corresponding to the $\bar{\Gamma}_A(\omega)$ in Fig. 4 and evaluated by means of Eq. (26). Though defined

as strain derivatives of the entropy [Eqs. (8)], it is thermodynamically equivalent to regard the Γ_A as a measure of the "thermal stress" developed on increasing the temperature at constant external and internal strain. This can be seen from the Maxwell relation

$$\left(\frac{\partial s}{\partial \epsilon_A}\right)_{s', T} = -V^0 \left(\frac{\partial T}{\partial T}\right)_s. \quad (28)$$

On the microscopic level this thermal stress is developed due to the increasing amplitude of the

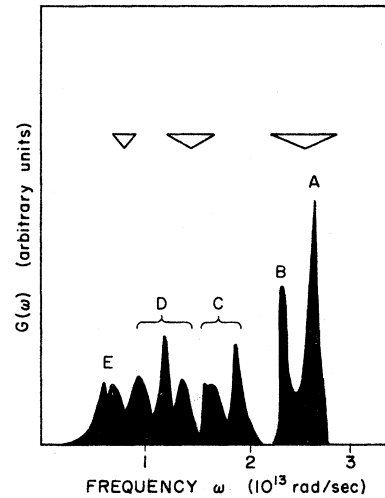


FIG. 3. Calculated harmonic-frequency spectrum obtained by root-sampling method. Triangles show the main peaks observed by Kotov *et al.* (Ref. 6). Different regions of the spectrum A-E are distinguished according to the dependence of the modes within them upon the harmonic force constants.

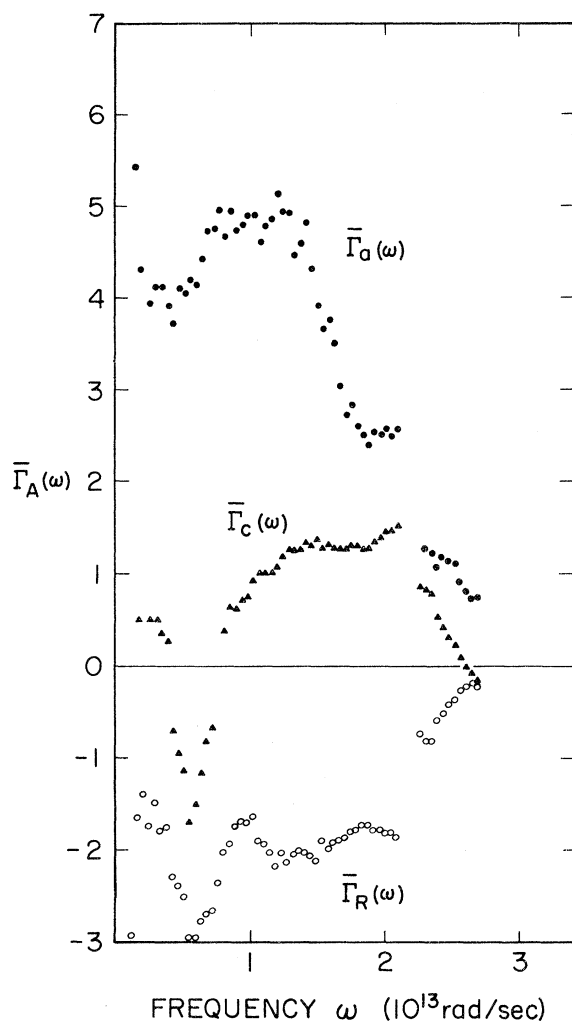


FIG. 4. Strain dependence of normal-mode frequencies in different regions of the frequency spectrum, expressed in the form of the quantities $\bar{\Gamma}_A(\omega)$. \bullet : $\bar{\Gamma}_a(\omega)$; \blacktriangle : $\bar{\Gamma}_c(\omega)$; \circ : $\bar{\Gamma}_R(\omega)$.

vibrations on excitation. To illustrate this point consider a linear chain of atoms with 6–12 nearest-neighbor pair potentials between neighbors. $\Gamma(\vec{q}, s)$ would be positive for a longitudinal mode since stretching the chain lowers the second derivatives of the potentials and hence the frequency. Considering now the chain held at constant length, as the longitudinal mode increases in amplitude the anharmonicity in the pair potentials creates a tendency for the mean interparticle distance to increase. This creates a thermal stress leading to an extension of the chain once the restriction of constant chain length is lifted.

When the solid is held at constant external and internal stress, the thermal stress developed on heating leads to a continual change in external and internal strain to an extent determined through

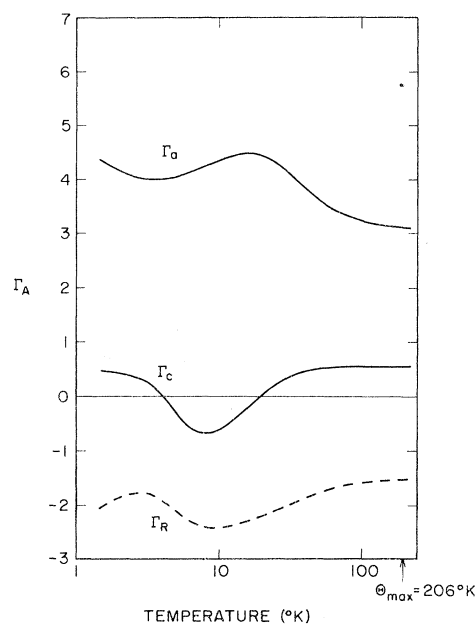


FIG. 5. Calculated Grüneisen functions Γ_A in the general regime plotted against $\log_{10} T$. $\Theta_{max} = \hbar\omega_{max}/k$ is indicated, where ω_{max} is the maximum calculated phonon frequency.

the elastic compliances s_{AB}^T . We thus arrive at Eq. (6) for the thermal expansion.

The Grüneisen functions γ_\perp and γ_\parallel in the macroscopic regime were calculated from Eqs. (9) and (10) and are shown as functions of temperature in Fig. 6. Under normal experimental conditions the internal stress is always zero so that γ_\perp and γ_\parallel describe the thermal pressure developed perpendicular and parallel to the unique axis after

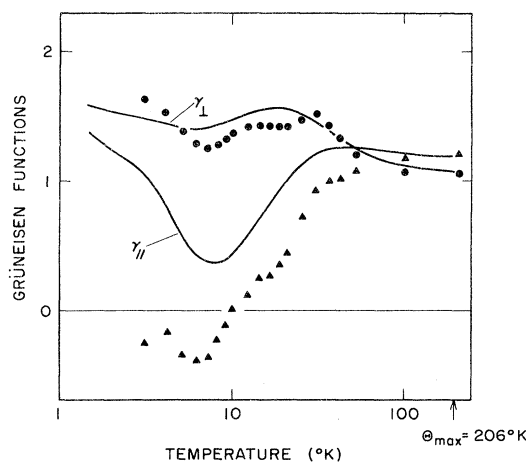


FIG. 6. Calculated Grüneisen functions γ_\perp and γ_\parallel (solid lines) in the macroscopic regime plotted against $\log_{10} T$. Graph also shows the values obtained experimentally by Ibach and Ruin (Ref. 14): \bullet : γ_\perp ; \blacktriangle : γ_\parallel .

allowing for relaxation of the internal thermal stress. Thus, the tendency of the chains to contract radially (Γ_R is negative over the whole range of temperature) to some extent "quenches" the thermal pressure perpendicular to the unique axis, so that $\gamma_\perp < \Gamma_a$ at all temperatures. However, interaction of the radius contraction through the cross stiffness c_{cR}^T leads to an expansive contribution to the thermal pressure along the chains, and hence $\gamma_\parallel > \Gamma_c$. (At low temperatures Γ_c is negative and so the chains want to contract along their length when held at constant radius. Internal relaxation of the chain radii thus opposes this contraction.)

The results for γ_\perp and γ_\parallel derived from experiment by Ibach and Ruin¹⁴ are also shown in Fig. 6 and one can see that the model reproduces the data quite well. The maximum in γ_\perp at $\sim 30^\circ\text{K}$ and the fluctuations below 10°K , particularly the minimum in γ_\parallel , are all reproduced by the model calculations (however, considerable uncertainty exists in the experimental points below 10°K). A measurement of the third-order elastic constants would be very useful in providing a "fix" on the low-temperature behavior of γ_\perp and γ_\parallel as $T \rightarrow 0^\circ\text{K}$.

The calculated thermal expansion coefficients a_\perp , a_\parallel , and α_R are plotted as functions of T in Fig. 7 together with the experimental data of Ibach and Ruin for a_\perp and a_\parallel . The graph also shows the value of α_R determined by Arnold and Grosse¹⁵ who used x rays to study the change in unit cell geometry between 300 and 500°K . The expansion perpendicular to the unique axis and the internal radial contraction of the chains are both fairly close to their experimental values. However, a_\parallel for the model becomes positive at $\sim 30^\circ\text{K}$ and is never less than $-2 \times 10^{-6}^\circ\text{K}^{-1}$ below this temperature, whereas experimentally a_\parallel is found to have a sharp minimum of $\sim -10 \times 10^{-6}^\circ\text{K}^{-1}$ at low temperatures and to remain negative as the temperature is raised. This discrepancy clearly indicates an inadequacy in the elastic properties of the model since γ_\perp and γ_\parallel for the model are in quite close agreement with experiment. It is easily shown²⁴ that a_\parallel only becomes positive if $\gamma_\parallel/\gamma_\perp > 2c_{13}^T/(c_{11}^T + c_{12}^T)$. This ratio is ~ 1.2 for tellurium whereas for the present model it is ~ 0.8 and hence a_\parallel becomes positive even before γ_\perp and γ_\parallel cross over.

Values for the force constants can be chosen to improve this ratio but they result in a worse fit to γ_\perp and γ_\parallel such that a_\parallel still becomes positive at high temperatures. This indicates that the internal elastic properties measured by c_{aR} , c_{cR} , and c_{RR} are then being incorrectly represented, particularly the former two since c_{RR} is directly related to the A_1 chain dilation frequency which is still quite well reproduced. This inadequacy arises because k_{ii} and k_{io} can only increase c_{13} through

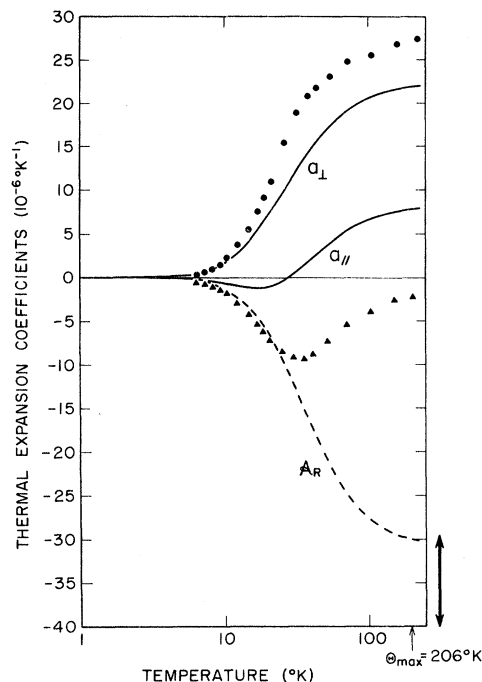


FIG. 7. Calculated external (solid lines) and internal (dashed line) thermal-expansion coefficients plotted against $\log_{10} T$. The experimental results of Ibach and Ruin (Ref. 14) are also shown. \bullet : a_\perp ; \blacktriangle : a_\parallel . The two-headed arrow indicates the value and estimated error for α_R measured by Arnold and Grasse (Ref. 15) using x-ray measurements between 300 and 500°K .

the ratio $c_{aR}c_{cR}/c_{RR}$ [see Eq. (14)] which then affects γ_\parallel and γ_\perp , whereas they make no contribution to c_{ac} since this stiffness arises from forces which depend to some extent on between-chain coordinates. The inadequacy with which such forces are represented is thus a conclusion which arises from comparison with both harmonic and anharmonic properties.

VII. SUMMARY AND DISCUSSION

The picture of the thermal expansion of tellurium suggested by this simple model is as follows: On heating, a thermal pressure is developed mainly between the helical chains, giving rise to a large positive expansion perpendicular to the unique axis. The elastic response to this expansion is to contract the crystal along the unique axis and at high temperatures this dominates any opposing axial thermal pressure to expand the chains. The thermal pressure developed in the nearest-neighbor between-chain "bonds" also serves to "push in" the chains so that their radii decrease and hence α_R is negative (this occurs since the internal degree of freedom allows the system to relax internally until the internal stress τ_R is zero). A further smaller contribution to the

negative α_R arises from the tendency of the in-chain angles to increase on heating.

As far as the model is concerned, it would seem that the most important contributions to the anharmonic terms in the lattice potential have been included and the model does not seem to suffer too much from the extremely simple way in which they are introduced. *However, comparison with both harmonic and anharmonic properties does indicate that the between-chain forces are too simply represented.* In addition to ϕ_b and ϕ_a , between-chain interactions must be included which improve the $c_{13}/(c_{11}+c_{12})$ ratio and reproduce the A_2 zone-center optic frequency without making $(c_{11}+c_{12})$ too large. Angle forces between in-chain and between-chain bonds may be the answer. The central interaction ϕ_a would then appear as a component of such forces, and they are certainly compatible with some degree of d^2sp^3 character in the bonding. The latter appears likely when one compares tellurium with the trends in structure and bonding observed for its neighbors in group VIb. Thus in the one extreme the various ring and chain structures of sulphur are compatible with a description of an sp^3 hybridized sulphur atom with two singly occupied orbitals, each forming a strong covalent bond with another sulphur atom and giving a bond angle close to the tetrahedral value of 109.5° . The bonding between the chains is very weak. In the series $S \rightarrow Se \rightarrow Te \rightarrow Po$ the bonding between the chains becomes progressively stronger relative to the within-chain binding; the in-chain bond angles decrease and the solids become more metallic, the last in the series, polonium, being a metal with the simple cubic structure.²⁹ The latter is not a normal structure for a metal and from a simple viewpoint might be derived from ds^2p^3 hybridized polonium atoms with six singly occupied orbitals, bonding to give octahedral coordination. While not compatible with the metallic nature of polonium this picture does explain the rather uncharacteristic structure for a metal and suggests that directional bonding would still be important. Coming just before polonium in group VIb therefore one would expect the bonding in tellurium to have some d^2sp^3 character. The availability of d orbitals for bonding certainly increases down the series. Indeed, the between-chain binding in tellurium is greater than expected for purely van der Waals interactions, which also suggests a weak overlap of bonding wave functions.

However, because electromagnetic interactions are not explicitly treated it is uncertain how much improvement in the model would be achieved by using a more sophisticated valence-force field as suggested above. Tellurium belongs to the simplest class of elemental crystals possessing a first-

order electric moment and as a result it exhibits one-phonon infrared absorption by the mechanism of displacement-induced charge redistribution. The effect of "dynamic charge" upon the lattice vibrations requires consideration of the polarizability of the atoms and this is clearly neglected in any valence-force approach. The work of Chen and Zallen³⁰ indicates that the A_2 frequency is particularly sensitive to this aspect of the interactions and as we have seen (Fig. 2), it is particularly hard to reproduce this frequency with the present model while still obtaining reasonable elastic constants.

Although the agreement with experimental measurements of the thermal expansion is remarkably good considering the simplicity of the model, improvements along the lines discussed above are clearly required and should be included in any more sophisticated treatment. It is felt that the present approach is justified as a first attempt because of the conceptually simple and straightforward way in which it deals with the anharmonic contributions to the lattice potential, and for the insight it gives into the physical mechanisms involved in the thermal expansion of tellurium.

On a more general note, one can see how the general thermodynamic formalism used in this paper enables one to get a feeling for the "internal" properties of a crystal, since it deals with them explicitly. Thus internal experimental measurements, such as those of α_R ,¹⁵ can be directly compared with model calculations.

It would be useful to obtain the Γ_A from measurements of a_\perp , a_\parallel , and α_R , since it is the Γ_A , and not γ_\perp and γ_\parallel , which are the quantities purely dependent on the anharmonic part of the lattice potential (see Sec. II). However, to derive the Γ_A one also needs to derive the c_g/C_η ratio and c_{AB}^T from experiment. The former can be taken to be unity with negligible error under most conditions but the latter requires knowledge of c_{RR}^T and the cross compliances s_{aR}^T and s_{cR}^T as well as the normal $c_{\lambda\mu}^T$ (see Ref. 21). c_{RR}^T can be obtained fairly accurately from measurements of the A_1 zone-center optic frequency. However, it is more difficult to determine s_{aR}^T and s_{cR}^T , which are a measure of how the internal strain ϵ_R varies with anisotropic stress applied perpendicular and parallel to the unique axis, and such measurements have not yet been carried out. They can be done in principle by uniaxial loading and the use of x rays (recently, changes in internal strain with isotropic pressure have been measured for selenium³¹). It would also be useful to measure α_R at temperatures lower than 300°K .

Finally, from the results for the tellurium model one can make some general remarks about the Grüneisen functions and thermal expansion of com-

plex crystals. By comparing the results for the Γ_A with those for γ_{\perp} and γ_{\parallel} one can see that one effect of having an internal degree of freedom has been to reduce the magnitude and anisotropy of the thermal pressure developed through the external strain coordinates. This is because *much of the thermal pressure developed is dissipated by internal rearrangement*. Such internal relaxation effects therefore account for the relatively small anisotropy of γ_{\perp} and γ_{\parallel} in tellurium despite the large elastic anisotropy. This apparent anomaly was pointed out by Munn³² in considering elastic effects in negative thermal expansion, but he

considered only the macroscopic γ_{\perp} and γ_{\parallel} , which as we have seen are not the fundamental theoretical quantities in crystals with internal degrees of freedom. The same effects may explain the anomalous case of arsenic raised by Munn, and also the low values of γ 's found for many complex crystals and glasses.

ACKNOWLEDGMENTS

I would like to thank Dr. T. H. K. Barron, Dr. R. W. Munn, and Dr. M. L. Klein for many helpful comments, and Dr. H. Ibach and M. Hortal for private communication of experimental results.

*Issued as NRCC report No. 12963.

¹P. Grosse, M. Lutz, and W. Richter, *Solid State Commun.* **5**, 99 (1967).

²G. Lucovsky, R. C. Keezer, and E. Burstein, *Solid State Commun.* **5**, 439 (1967).

³B. H. Torrie, *Solid State Commun.* **8**, 1899 (1970).

⁴A. S. Pine and G. Dresselhaus, *Phys. Rev. B* **4**, 356 (1971).

⁵B. M. Powell and P. Martel, *Proceedings of the Tenth International Conference on the Physics of Semiconductors, Cambridge, Mass., 1970* (U.S. AEC, Technical Information Div., Oak Ridge, Tenn., 1970).

⁶B. A. Kotov, N. M. Okuneva, and A. L. Shakh-Budagov, *Fiz. Tverd. Tela* **9**, 2553 (1967) [*Sov. Phys. Solid State* **9**, 2011 (1968)].

⁷W. Gissler, A. Axmann, and T. Springer, *Neutron Inelastic Scattering* (International Atomic Energy Agency, Vienna, 1968), Vol. 1, p. 245.

⁸J. L. Malgrange, G. Quentin, and J. M. Thuiller, *Phys. Stat. Sol.* **4**, 139 (1964).

⁹W. DeSorbo, *J. Chem. Phys.* **21**, 764 (1953).

¹⁰P. L. Smith, *Conférence de Physique des Basses Températures* (Institute de International du Froid, Paris, 1955), p. 281.

¹¹T. Fukuroi and Y. Muto, *Sci. Rep. Res. Inst. Tohoku Univ.* **A8**, 213 (1956).

¹²A. K. White, *J. Phys. C Lett.* (to be published).

¹³S. I. Novikova, *Fiz. Tverd. Tela* **10**, 3439 (1968) [*Sov. Phys. Solid State* **10**, 2723 (1969)].

¹⁴H. Ibach and R. Ruin, *Phys. Stat. Sol.* **41**, 719 (1970).

¹⁵J. U. Arnold and P. Grosse, *Phys. Stat. Sol.* **28**, K93 (1968).

¹⁶S. Ahmed and S. Weintraub, Univ. of Southampton (private communication).

¹⁷M. Hortal, Univ. of Bristol (private communication).

¹⁸M. Hulin, *Ann. Phys. (Paris)* **8**, 647 (1963).

¹⁹R. Geick and U. Schröder, *The Physics of Selenium and Tellurium*, edited by W. C. Cooper (Pergamon, New York, 1969), p. 277.

²⁰T. Nakayama, Y. Ikeda, and A. Odajima, *J. Phys. Soc. Japan* **30**, 885 (1971).

²¹T. H. K. Barron, T. G. Gibbons, and R. W. Munn, *J. Phys. C* **4**, 2805 (1971).

²²G. Liebfried and W. Ludwig, *Solid State Phys.* **12**, 276 (1961).

²³T. G. Gibbons, Ph.D. thesis (University of Bristol, 1971) (unpublished).

²⁴T. H. K. Barron and R. W. Munn, *Phil. Mag.* **15**, 85 (1967).

²⁵M. Blackman, *Proc. Phys. Soc. (London)* **B70**, 827 (1957).

²⁶C. Kittel, *Quantum Theory of Solids* (Wiley, New York, 1963), p. 214.

²⁷T. H. K. Barron, *J. Appl. Phys.* **41**, 5044 (1970).

²⁸T. H. K. Barron and T. G. Gibbons (unpublished).

²⁹A. Von Hippel, *J. Chem. Phys.* **16**, 372 (1948).

³⁰I. Chen and R. Zallen, *Phys. Rev.* **173**, 833 (1968).

³¹D. McCann and L. Cartz, Marquette University (unpublished).

³²R. W. Munn, *J. Phys. C* **5**, 535 (1972).